

**DYNAMICAL BEHAVIORS ANALYSIS
AND NUMERICAL SIMULATION OF THE
LORENZ-TYPE SYSTEM FOR COUETTE-TAYLOR FLOW**

HEYUAN WANG

College of Sciences, Liaoning University of Technology, Jinzhou 121001, China

ABSTRACT. In this paper, we investigate the problem of dynamical behaviors and numerical simulation of the Lorenz-type systems for the incompressible flow between two concentric rotating cylinders. The estimation of Hausdorff dimension of its attractor is discussed, and the globally exponentially attractive set and positive invariant set of the chaotic system are studied via Lyapunov function. We present a detailed numerical result of the whole process from bifurcation to chaos, and analyze the evolutionary mechanism of the dynamical behavior of the system. Moreover, by using numerical simulation results of attractors, bifurcation diagram, Lyapunov exponent spectrum and Poincare map, return map of the system we show abundant and complex dynamical behaviors of the system, and explain successive transitions of Couette-Taylor flow from Laminar flow to turbulence in the experiment.

Key Words Couette-Taylor flow, the Lorenz system, attractor, Poincare map.

1. Introduction

There have been a lot of investigations which concern with rotating flow between two concentric cylinders (abbreviate frequently as Couette-Taylor Flow), and Couette-Taylor flow is the typical rotation flow problems, it provides a paradigm from laminar to turbulent transition, and we refer the readers to [1–12]. The outer cylinder is fixed while the inner cylinder rotates at a constant angular velocity ω , when ω is small, the basic flow is the Couette flow consisting of current lines which are coaxial circles. When ω exceeded a critical value ω_{1c} , this basic flow becomes unstable and a new complicated flow is observed, and it is axisymmetric and stationary, called the Taylor vortices (the Taylor vortex flow). In fact, this is a bifurcation phenomenon, mathematically, the instability represents a supercritical steady bifurcation from Couette flow to Taylor vortex flow. This regime is still stationary, and the rotational invariance of the flow is not broken. The second transition breaks both the time and rotational symmetry, the regime is now periodic and the cells assume a wavy

Supported by the Natural Science Foundation of China (11572146), scientific research foundation of education department of Liaoning province (L2013248) and science and technology funds of Jinzhou city (13A1D32)

form. These waves move uniformly about the Z-axis, so that in a suitable rotating frame, the flow appears stationary. Such periodic motions are called rotating waves. The third transition leads to a quasi-periodic flow, which are called modulated wavy Taylor vortices. Subsequent bifurcations follow several possible routes but generally lead to turbulence after a few steps. When both cylinders are rotated in opposite directions, even richer “routes” to turbulence are observed. Previous research work mostly focused on the stability and bifurcation theory of the flow, It is mainly used to explain and analyze the various kinds of vortex and the evolution process of the various vortices in the experiment, as well as the way of the transition from laminar flow to turbulent flow, and the existence and simulation of chaotic attractors of the turbulent state are rarely involved in the literature. As the global attractor of the Couette-Taylor flow between two concentric cylinders is very complex and difficult of simulation, and the occurrence of turbulence is usually derived from instability of a small number of modes, we use the simplified mode analysis method for numerical simulation. Low-dimensional analysis of fluid systems are of interest in order to capture the essential of their behavior, the theoretical basis is theory of the inertial manifold and approximate inertial manifold (they are considered to be a low dimensional smooth manifold containing the global attractor and the exponential attractor of all orbits), namely, the complicated dynamical behavior of the infinite dimensional dynamical systems can arise from a few simple coupled ordinary, and be distinguished by the simple equations. This simplified mode analysis method not only can overcome the troublesome difficulty of the Couette-Taylor flow problem, but also involve some essential features of the flow, which is very meaningful to discuss nonlinear phenomena of Navier-Stokes equation, for example, the bifurcation, turbulence etc. Although the dynamic behavior of the Lorenz-type equation is not exactly the same as the actual flow of the Couette-Taylor flow, it can not only achieve the minimum degree of freedom of simulation but also reflect some essential features of the flow, this is a valuable attempt to use the simple model to reflect some of the features of complex problems. Of course, the fascinating and confusion vortex wave observed in the experiment before the occurrence of turbulence may be beyond the expressed scope of finite model Lorenz-type equations, so we can't expect to obtain all the details of this complex problem, the focus of our study is interpretation of three typical flow of the Couette-Taylor flow before evolution into turbulence and some features of the turbulence behavior after flow transition to chaos and its simulation. Chen and Hsien [1987] investigated a model system of evolutionary equations for axisymmetric Couette-Taylor flow, but the model of truncation seemed too simple, there were no Hopf bifurcation and chaos behaviors in their system. Heyuan Wang [2012] derive a three-model system by using spectral Galerkin method, and discover chaos phenomena. The existence of its attractor was given, some numerical simulation results

were presented [Heyuan Wang 2012]. In this paper, we further study dynamical behaviors of the three-model Lorenz-type system, discuss the estimation of Hausdorff dimension of its attractor, and present numerical simulation results of attractors, bifurcation diagram, Lyapunov exponent spectrum, Poincare map and return map of dynamical behaviors. The outline of the paper is as follows. In section 2 we discuss the estimation of Hausdorff dimension of its attractor. In section 3 we study the globally exponentially attractive set and positive invariant set of the three-mode system. In section 4 we present numerical simulation results of attractors, bifurcation diagram, Lyapunov exponent spectrum, Poincare map and return map of the system, and analyze the evolutionary mechanism of the dynamical behavior of the system.

2. The three-mode Lorenz-type equation and the estimation of Hausdorff dimension of its attractor

Heyuan Wang introduce eigenfunctions of Stokes operator in the cylindrical gap regions as basis function of Fourier expansions, and derive the following three-model Lorenz-type system by a suitable model truncation of the Navier-Stokes equations for the incompressible flow between two concentric rotating cylinders in periodic boundary conditions in the Z-axis [Heyuan Wang 2012]

$$(2.1) \quad \begin{cases} \dot{X} = -C_1X + C_2ReZ - C_3YZ, \\ \dot{Y} = -C_4Y + C_5XZ, \\ \dot{Z} = C_6RX - C_7Z - C_8XY. \end{cases}$$

where Re is Reynolds number, X, Y, Z is Fourier coefficients, they are function of t , and C_1, \dots, C_8 are positive parameter. The model equations (2.1) are the same as the model system of Chen and Hsien [1987], which is a Lorenz-type system. Because the coefficients satisfy $C_1 + C_4 > C_7$ in the model system of Chen and Hsien [1987], there is no Hopf bifurcation even for large Reynolds number Re . On the contrary, due to disappearance of the restricted condition $C_1 + C_4 > C_7$ in the model system (2.1), there exists Hopf bifurcation and chaos [Heyuan Wang 2012].

For the system (2.1) there exists trivial stationary solution $O = (0, 0, 0)$ and two nontrivial stationary solutions P_+, P_- [Heyuan Wang 2012]. In order to discuss the stability of the nontrivial stationary solutions P_{\pm} Heyuan Wang [2012] introduces the following transformation:

$$(2.2) \quad \begin{cases} t = s\tau, \\ X = s_2y, \\ Y = s_3z, \\ Z = s_1x. \end{cases}$$

Due to $C_3C_5 > 0$, $C_6 \neq 0$, we set $s = \frac{1}{C_1}$, $s_1 = \frac{C_1}{\sqrt{C_3C_5}}$, $s_2 = \frac{C_1C_7}{C_6\sqrt{C_3C_5}Re}$, $s_3 = \frac{C_1C_7}{C_3C_6Re}$, then (2.1) can be rewritten as a Lorenz-type system:

$$(2.3) \quad \begin{cases} \dot{x} = -\sigma(x - y) + cyz, \\ \dot{y} = -xz + rx - y, \\ \dot{z} = xy - bz, \end{cases}$$

where $r = \frac{C_2C_6}{C_1C_7}Re^2$, $c = \frac{C_7^2C_8}{C_6^2C_3Re^2}$, $b = \frac{C_4}{C_1}$, $\sigma = \frac{C_7}{C_1}$. In contrast to Lorenz system, the system (2.3) has an additional nonlinear term cyz .

In the following we discuss the estimation of Hausdorff dimension of its attractor. Fixing x, y , replacing z with $z + \sigma + r$, and setting $p_0 = [\sigma + c(r + \sigma)]$, we rewrite system (2.3) as

$$(2.4) \quad \begin{cases} \dot{x} = -\sigma x + p_0 y + cyz & (1) \\ \dot{y} = -xz - \sigma x - y & (2) \\ \dot{z} = xy - bz - b(r + \sigma) & (3). \end{cases}$$

Let E be Hilbert space, and $Y \subset E$ be a subset of E , I be index set. Given $d \in R_+$, $\epsilon > 0$, we denote by $\mu_H(Y, d, \epsilon)$ the quantity $\inf \sum_{i \in I} r_i^d$, r_i be radius of a family ball covering Y of E , and $r_i \leq \epsilon$ (for all $i \in I$). Set

$$\mu_H(Y, d) \triangleq \lim_{\epsilon \rightarrow 0} \mu_H(Y, d, \epsilon) = \sup_{\epsilon > 0} \mu_H(Y, d, \epsilon)$$

$\mu_H(Y, d)$ is called d -dimensional Hausdorff measure of Y .

There exists $d_0 \in [0, \infty)$ such that $\mu_H(Y, d) = 0$ for $d > d_0$, $\mu_H(Y, d) = +\infty$ for $d < d_0$, the number d_0 is called the Hausdorff dimension of Y , and is denoted $d_H(Y)$ (R. Temam [12]), and the following conclusion is quoted from R. Temam [12].

Theorem 2.1. *Let H be a Hilbert space, and $X \subset H$ be a compact set, and S be a continuous mapping from X into H such that $SX \subset X$. We assume that L is "uniformly differentiable on X ", i.e., For every $u \in X$, there exists a linear operator $L(u) \in L(H)$ and*

$$\sup_{\forall u, v \in X, 0 < |u-v|_X < \epsilon} \frac{\|Su - Sv - L(u)(v - u)\|}{\|u - v\|} \rightarrow 0, \quad \text{as } \epsilon \rightarrow 0$$

where $\|\cdot\|, |\cdot|_X$ are norm of H and X respectively, and we assume the following:

$$\sup_{\forall u \in X} \|L(u)\|_{L(H)} < +\infty,$$

$$\sup_{\forall u \in X} \omega_d(L(u)) < 1 \quad \text{for some } d > 0,$$

then the Hausdorff dimensional of X is less than or equal to d .

We present estimation of Hausdorff dimension of attractor in the following conclusion, in the proof of the following theorem 1 we refer to the method shown in literature [12], but we have discovered a few mistakes in the process of proof in literature [12], we have revised these errors. Since our system contains the cyz , the following discussion become more complicated. Definition of $\omega_d, \omega_m(L), \alpha_m(L), \bigwedge^m H, (\cdot, \cdot)_{\bigwedge^m H}$ is quoted from R. Temam [12],

Theorem 2.2. *For three-mode equations (2.3) Hausdorff dimension of its attractor satisfies $d_H \leq 2 + s$, and $s \in (0, 1)$.*

Proof. System (2.4) can be written in the form

$$\frac{du}{dt} = F(u) = F(x, y, z) = - \begin{pmatrix} \sigma x - p_0 y - cyz \\ \sigma x + y + xz \\ bz - xy + b(r + \sigma) \end{pmatrix}.$$

Let $U = \xi(t) \in H = R^3$, and we consider the following initial-value problem

$$(2.5) \quad \begin{cases} \frac{dU}{dt} = F'(u) \cdot U \\ U(0) = \xi, \\ -F'(u) \cdot U = A_1 U + A_2 U + B(u)U, \end{cases}$$

where

$$A_1 = \begin{pmatrix} \sigma & 0 & 0 \\ 0 & 1 & 0 \\ 0 & 0 & b \end{pmatrix}, \quad A_2 = \begin{pmatrix} 0 & -\sigma & 0 \\ \sigma & 0 & 0 \\ 0 & 0 & 0 \end{pmatrix},$$

$$B(u) = \begin{pmatrix} 0 & -c(r + \sigma) - cz & -cy \\ z & 0 & x \\ -y & -x & 0 \end{pmatrix}, \quad \forall u = (x, y, z) \in R^3.$$

For initial-value $\xi_1, \xi_2, \xi_3 \in R^3$, solution $U = (U_1, U_2, U_3)$ of the initial-value problem (2.5) satisfies $U_i(t) = L(t, u_0)\xi_i, \forall t > 0$. u_0 is stationary solution of the system (2.4). $L(t, u_0)$ is linear operator from R^3 into R^3

$$L(t, u_0) : U(0) = \xi(\in R^3) \rightarrow U(t)(\in R^3).$$

In $\bigwedge^m H (m = 2, 3)$ we consider

$$\frac{d}{dt} |U_1 \wedge U_2 \wedge U_3| = |U_1 \wedge U_2 \wedge U_3| \text{Tr} F'(u)$$

$$\frac{d}{dt} |U_1 \wedge U_2| = |U_1 \wedge U_2| \text{Tr}(F'(u) \cdot Q),$$

where $Q = Q_2(t, u_0; \xi_1, \xi_2)$ is orthogonal projection from R^3 into $\overline{\text{span}\{U_1, U_2\}}$, notation Tr is quoted from R. Temam [12].

$$|U_1 \wedge U_2 \wedge U_3(t)| = |\xi_1 \wedge \xi_2 \wedge \xi_3| \exp[-(\sigma + b + 1)t]$$

$$\omega_3(L(t, u_0)) = \sup_{\xi_i \in H, |\xi|=1, i=1,2,3} |U_1 \wedge U_2 \wedge U_3(t)|$$

therefore, $\omega_3(L(t, u_0)) \leq \exp[-(\sigma + b + 1)t]$.

Let $\Lambda_i, \mu_i (i = 1, 2, 3)$ be uniform Lyapunov numbers and uniform Lyapunov exponents (R. Temam [12]), then

$$\Lambda_1 \Lambda_2 \Lambda_3 = \lim_{t \rightarrow \infty} \overline{\omega_3(t)}^{1/t} = \exp[-(\sigma + b + 1)],$$

$$\mu_1 + \mu_2 + \mu_3 = -(\sigma + b + 1).$$

By similar manner we have

$$|U_1 \wedge U_2| = |\xi_1 \wedge \xi_2| \exp \int_0^t \text{Tr}(F'(u(c)) \cdot Q(c)) dc.$$

Assume that $|\xi_1 \wedge \xi_2| \neq 0$, thus $|U_1 \wedge U_2| \neq 0, \forall t > 0$.

$$\text{Tr}(A_1 + A_2) \cdot Q = \text{Tr}(A_1) \cdot Q \geq 1 + b + \sigma - m$$

where $m = \max(1, b, \sigma)$.

Set $\varphi_i = (x_i, y_i, z_i), i = 1, 2, 3$ be an orthogonal basis of R^3 , thereafter $x_1 y_1 + x_2 y_2 = -x_3 y_3$. We find

$$\begin{aligned} \text{Tr}(B(u) \cdot Q) &= \sum_{i=1}^2 (B(u) \varphi_i) \varphi_i \\ &= \sum_{i=1}^2 [(-c z x_i y_i - c y x_i z_i + z x_i y_i + x y_i z_i - y x_i z_i - x y_i z_i) - c(r + \sigma) x_i y_i] \\ &= \sum_{i=1}^2 [(1 - c) z x_i y_i + (-1 - c) y x_i z_i - c(r + \sigma) x_i y_i] \\ &= -(1 - c) z x_3 y_3 + (1 + c) y x_3 z_3 + c(r + \sigma) x_3 y_3. \end{aligned}$$

When $c \leq 0$, we have $1 - c \geq |1 + c|$, then

$$\begin{aligned} \text{Tr}(B(u) \cdot Q) &= -(1 - c) z x_3 y_3 + (1 + c) y x_3 z_3 + c(r + \sigma) x_3 y_3 \\ &\leq |x_3| |1 - c| \sqrt{z^2 + y^2} \sqrt{y_3^2 + z_3^2} + |c(r + \sigma)| \\ &\leq \frac{1}{2} |1 - c| \sqrt{y^2 + z^2} + |c(r + \sigma)| \\ &\leq \frac{1}{2} |1 - c| |u(t)| + |c(r + \sigma)|, \end{aligned}$$

where $|u(t)| = \sqrt{x^2 + y^2 + z^2}, |\varphi_i| = \sqrt{x_i^2 + y_i^2 + z_i^2}$.

Therefore $\text{Tr}(B(u) \cdot Q) \geq -\frac{1}{2}(1 - c)\rho_0 - \delta$, where ρ_0 is absorbing radius of the system when $c < 0 (0 < \delta \ll 1)$.

Thereafter $|U_1 \wedge U_2| \leq |\xi_1 \wedge \xi_2| \exp((k_2 + \delta)t)$, where $k_2 = -(\sigma + b + 1) + m + \frac{1}{2}\rho_0(1 - c) + |c(r + \sigma)|$, therefore

$$\begin{aligned}\omega_2(L(t, u_0)) &\leq \exp((k_2 + \delta)t) \quad t \geq t_1(\delta), \\ \overline{\omega_2(t)} &\leq \exp((k_2 + \delta)t), \\ \Lambda_1 \Lambda_2 &\leq \exp(k_2), \\ \mu_1 + \mu_2 &< k_2.\end{aligned}$$

Assume that $d_H = 2 + s$, $0 < s < 1$, $t \geq t_1(\delta)$, we get

$$d_H = 2 + s \leq 2 + \frac{k_2 + \delta}{\sigma + b + 1 + k_2 + \delta}.$$

When $c \geq 0$, estimate is different slightly, namely,

$$\begin{aligned}|Tr(B(u) \cdot Q)| &\leq |-(1 - c)x_3y_3 + (1 + c)yx_3z_3| + |c(r + \sigma)| \\ &\leq \frac{1}{2}(1 + c)|u(t)| + |c(r + \sigma)|.\end{aligned}$$

Accordingly, $Tr(B(u) \cdot Q) \geq -\frac{1}{2}(1 + c)\rho_0 - \delta$, therefore, $k'_2 = -(\sigma + b + 1) + m + \frac{1}{2}\rho_0(1 + c)$, then $d_H = 2 + s \leq 2 + \frac{k'_2 + \delta}{k'_2 + \delta + \sigma + b + 1}$.

We complete estimation of Hausdorff dimension of attractor. \square

3. The globally exponentially attractive set and positive invariant set

In order to study the globally exponentially attractive set and positive invariant set of the three-mode Lorenz-type system we rewrite system (2.3) as

$$(3.1) \quad \begin{cases} \dot{x} = -\sigma(x - y) + \frac{c}{r}yz, \\ \dot{y} = -xz + arx - y, \\ \dot{z} = xy - bz, \end{cases}$$

where $a = \frac{C_2C_6}{C_1C_7}$, $c = \frac{C_7^2C_8}{C_6^2C_3}$, $b = \frac{C_4}{C_1}$, $\sigma = \frac{C_7}{C_1}$, $r = Re^2$. First, we present a basic definition here, let $X = (x, y, z)$ and suppose $X(t) = X(t, t_0, X_0)$ is a solution of system (3.1), and we denote the solution of system (3.1) satisfying the initial value $X(t_0, t_0, X_0) = X_0$.

Definition 3.1. If there exists a constant number $L > 0$ such that for $V(X_0) > L$, $V(X(t)) > L$, imply $\lim_{t \rightarrow +\infty} V(X) \leq L$, then $\Omega = \{X \mid V(X(t)) \leq L\}$ is said to be a globally attractive set of system (3.1).

Definition 3.2. If for any $X_0 \in \Omega$ and any $t > t_0$, imply $X(t, t_0, X_0) \in \Omega$, then $\Omega = \{X \mid V(X(t)) \leq L\}$ is said to be positive invariant set.

Definition 3.3. If there exists constant numbers $L > 0$, $M > 0$ and any $X_0 \in R^3$ such that for $V(X_0) > L$, $V(X(t)) > L$, imply the following exponentially estimate inequality: $V(X(t)) - L \leq (V(X_0) - L)e^{-M(t-t_0)}$, then $\Omega = \{X \mid V(X(t)) \leq L\}$ is said to be a globally exponentially attractive set of system (3.1).

Theorem 3.4. *Let*

$$(3.2) \quad V = x^2 + \left(1 + \frac{c}{r}\right) y^2 + \left[z - \sigma - \left(1 + \frac{c}{r}\right) ar\right]^2$$

$$(3.3) \quad L = \frac{b^2[\sigma + (1 + \frac{c}{r})ar]^2}{2b - 1}$$

when $V(X_0) \geq L$, and $V(X(t)) \geq L$, then system (3.1) has the following estimate inequality for globally exponentially $V(X(t)) - L \leq (V(X_0) - L)e^{-(t-t_0)}$, and $\overline{\lim}_{t \rightarrow +\infty} V(X(t)) \leq L$. i.e. $\Omega = \{X \mid V(X(t)) \leq L\}$ is the globally exponentially attractive set and positive invariant set of the system (3.1).

Proof. We construct a family of generalized radically infinite and positive definite Lyapunov functions as

$$V = x^2 + \left(1 + \frac{c}{r}\right) y^2 + \left(z - \sigma - \left(1 + \frac{c}{r}\right) ar\right)^2$$

Computing the time derivative along the positive half-trajectory of system (3.1), we have

$$(3.4) \quad \dot{V} = 2x\dot{x} + 2\left(1 + \frac{c}{r}\right) y\dot{y} + 2\left[z - \sigma - \left(1 + \frac{c}{r}\right) ar\right] \dot{z} = -V + F(X)$$

where

$$\begin{aligned} F(X) = F(x, y, z) &= (1 - 2\sigma)x^2 - \left(1 + \frac{c}{r}\right) y^2 - (1 - 2b)z^2 \\ &\quad - 2\left[\sigma + \left(1 + \frac{c}{r}\right) ar\right] (1 - b)z + \left[\sigma + \left(1 + \frac{c}{r}\right) ar\right]^2. \end{aligned}$$

Because $F(x, y, z)$ is quadratic function, its local maximum is the global maximum.

Let

$$\begin{aligned} \frac{\partial F}{\partial x} &= 2(1 - 2\sigma)x = 0, \\ \frac{\partial F}{\partial y} &= -2\left(1 + \frac{c}{r}\right) y = 0, \\ \frac{\partial F}{\partial z} &= 2(1 - 2b)z - 2\left[\sigma + \left(1 + \frac{c}{r}\right) ar\right] (1 - b) = 0, \end{aligned}$$

we have $x = 0$, $y = 0$, $z = \frac{[\sigma + (1 + \frac{c}{r})ar](1-b)}{1-2b}$, then we obtain the following two-order derivative of $F(X)$ at the point $\left(0, 0, \frac{[\sigma + (1 + \frac{c}{r})ar](1-b)}{1-2b}\right)$,

$$\begin{aligned} \frac{\partial^2 F}{\partial x^2} &= 2(1 - 2\sigma) < 0, \quad \text{when } \sigma > \frac{1}{2}, \\ \frac{\partial^2 F}{\partial y^2} &= -2\left(1 + \frac{c}{r}\right) < 0, \quad \text{when } \left(1 + \frac{c}{r}\right) > 0, \end{aligned}$$

$$\frac{\partial^2 F}{\partial z^2} = 2(1 - 2b) < 0, \quad \text{when } b > \frac{1}{2},$$

$$\frac{\partial^2 F}{\partial x \partial y} = \frac{\partial^2 F}{\partial y \partial z} = \frac{\partial^2 F}{\partial z \partial x} = 0.$$

So

$$\begin{aligned} \sup_{X \in R^3} F(X) &= F(X) \Big|_{(x=0, y=0, z = \frac{[\sigma + (1 + \frac{c}{r}) ar](1-b)}{1-2b})} \\ &= \frac{b^2 [\sigma + (1 + \frac{c}{r}) ar]^2}{2b - 1} = L \end{aligned}$$

From (3.4), we have $\frac{dV}{dt} \leq -V + L$, and we get the following globally exponentially estimate $V(X(t)) - L \leq (V(X_0) - L)e^{-(t-t_0)}$, when $V(X_0) \geq L$, $V(X(t)) \geq L$, and we take the upper limit of the both sides for $V(X(t)) - L \leq (V(X_0) - L)e^{-(t-t_0)}$, then $\overline{\lim}_{t \rightarrow +\infty} V(X(t)) \leq L$. Therefore, $\Omega = \{X \mid V(X(t)) \leq L\}$ is the globally exponentially attractive set and positive invariant set of the system (3.1). \square

4. The Numerical Simulation and Analysis of Dynamical Behaviors

Heyuan Wang obtains the following concrete three-mode equations [Heyuan Wang 2012]

$$(4.1) \quad \begin{cases} \dot{x} = -4.52(x - y) + \frac{1.843}{r}yz, \\ \dot{y} = -xz + 1.723rx - y, \\ \dot{z} = xy - 1.436z. \end{cases}$$

The numerical computation results indicate that system (4.1) has complicated dynamical behaviors with increasing the parameter $r = Re^2$. In this section we present the numerical experiment results.

1) For $0 < r < r_1 = 1.263 \dots$, the stationary solutions O of system (4.1) is stable, in this case O is the only attractor of the system. As r passes through r_1 , equilibrium solutions O becomes unstable, simultaneous with the loss of stability of O , the two fixed points P_{\pm} are born, for $r_1 \leq r < 4.515 \dots$, the stationary solutions P_{\pm} of system (4.1) is stable, Numerical evidences indicate that any randomly chosen initial data is attracted by one of them, so they are global attractors (see Fig. 1, 2).

2) At $r = 4.515 \dots$ the two stable stationary solutions P_{\pm} become unstable because a pair of complex conjugate eigenvalues of Jacobian matrix at stationary point P_{\pm} crosses the imaginary axis, each of the two stable stationary solutions P_{\pm} loses stability undergoing a Hopf bifurcation, and each generates a unstable periodic orbit (Fig. 3).

3) At $r = 4.615 \dots$, the unstable periodic orbits gives rise to a new orbit, the new orbits wind up around two of the stationary solutions P_{\pm} , instead of only one like the previous ones (Fig. 4), the motions become more and more complicate as r grows,

eventually generating a chaotic attracting set, namely, the strange attractor appears (Fig. 5–10).

4) For $24.714 < r < 30.713\dots$, the strange attractor shrinks into a limit cycles gradually (Fig. 11–15), if followed backwards with decreasing r , this bifurcation is an “inverse” bifurcation.

5) For $30.721 < r < 36.981\dots$, increasing r we found further bifurcation points, since the orbits become increasingly intricate requiring higher precision, we did not look for further bifurcations. So we cannot definitely state whether we have just a finite number of bifurcations and the only obstacle to observe more seems to be the numerical precision needed, then the strange attractor appears again, Fig. 16–18 presents three kinds of quasi-periodic state, Fig. 19,20 describes two kinds of attractor in different r . With the increasing of the parameter r , a strong hysteresis phenomenon(i.e., coexistence of stable attractors) appears, in some intervals hysteresis takes place between closed orbits and tori (Fig. 21–35).

6) Fig. 36 shows bifurcation diagrams of the system (4.1), Fig. 37 are the corresponding largest Lyapunov exponents, we can see that region of the positive maximum Lyapunov exponents in Fig. 37 and chaotic region of the bifurcation Fig. 36 is consistent.

7) Fig. 38 shows Poincare section of the system (4.1) ($r = 34.894$); Fig. 39 shows return map of the system (4.1) ($r = 14.894$); Fig. 40 present the power spectrum of the system (4.1), they indicate that chaos feature of the system (4.1).

8) From bifurcation diagrams Fig. 36 we find that the chaotic region contains periodic-orbit windows of varying width, the strange attractors and limit cycles appear alternately at some parameter r . Through more delicate and difficult calculation we obtain the following details: at $r = 30.713\dots$ and $r = 42.855\dots$ the strange attractor shrinks into a limit cycles(Fig. 14, 15, 24), at $r = 30.721\dots$ and $r = 44.785\dots$ the limit cycles become unstable and the periodic orbits generated by the period doubling bifurcation continue to double in ever faster succession eventually generating a chaotic attracting set (Fig. 16–20) at $r = 224.895\dots$ the limit cycles gradually evolved into a torus (Fig. 29–35), if followed backwards with decreasing r , this bifurcation is an “inverse” bifurcation (Fig. 36).

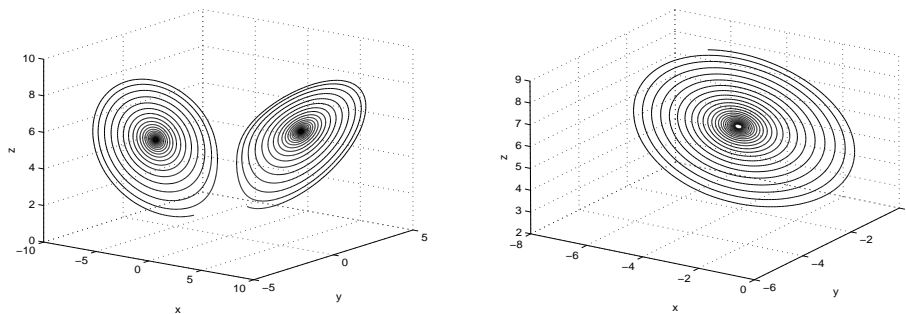
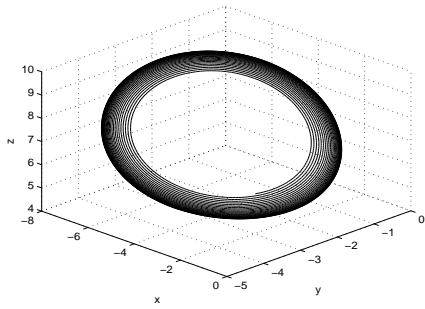
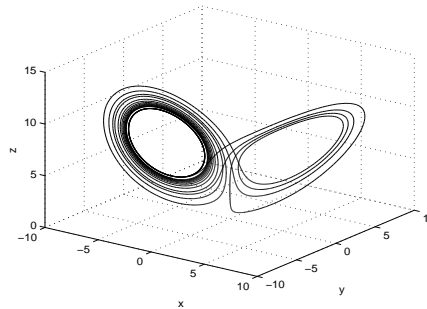
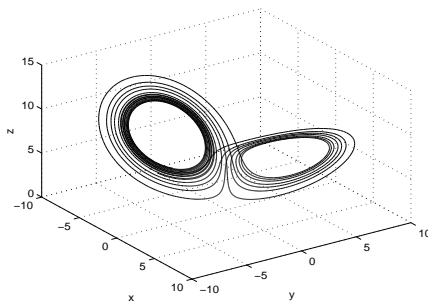
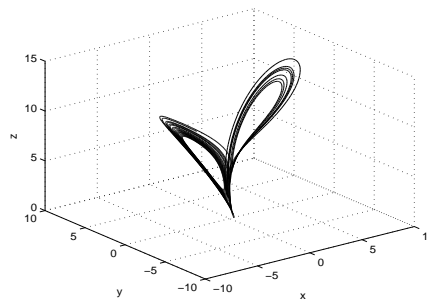
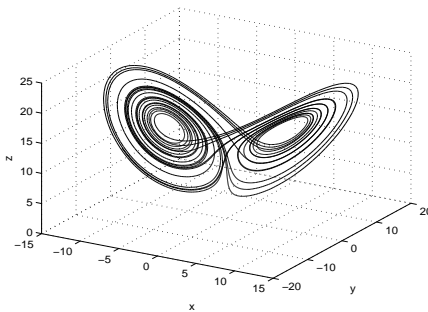
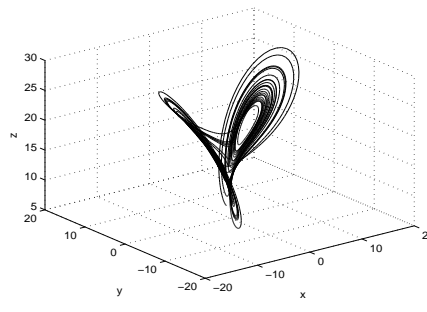
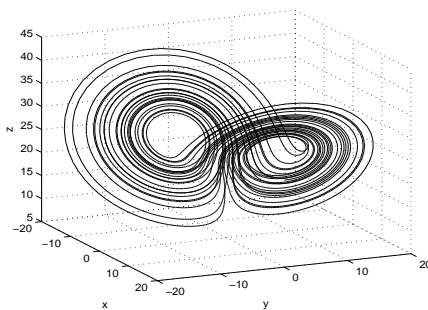
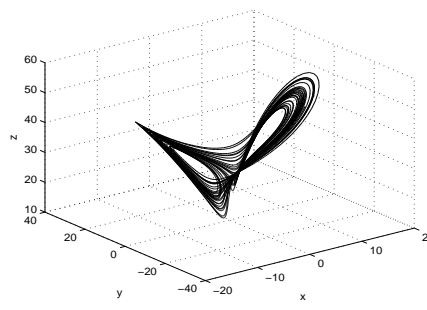
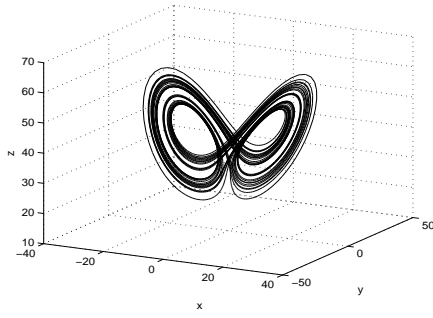
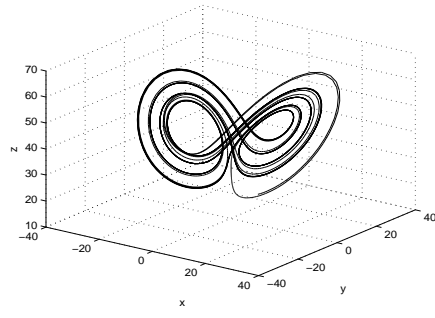
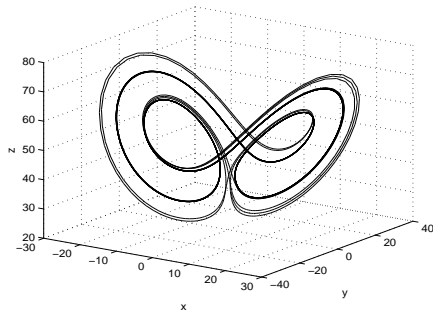
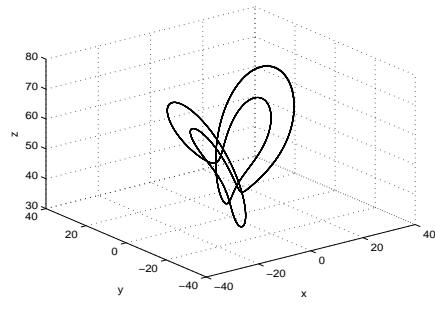
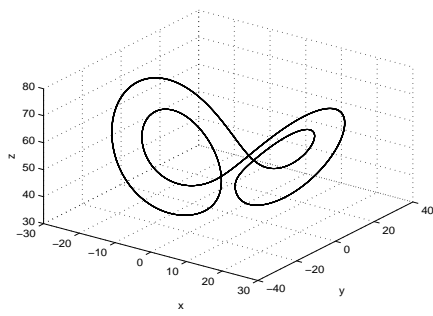
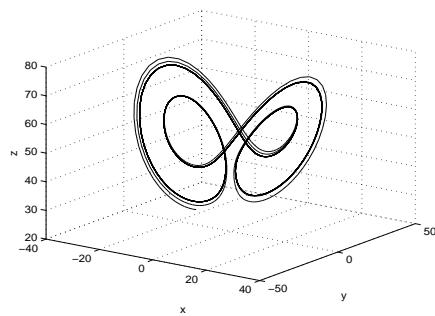
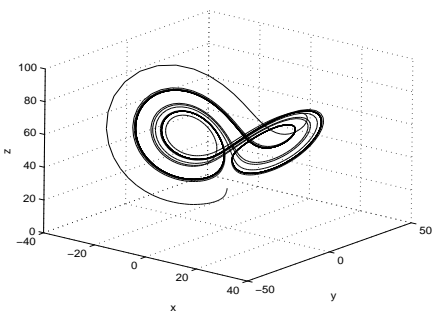
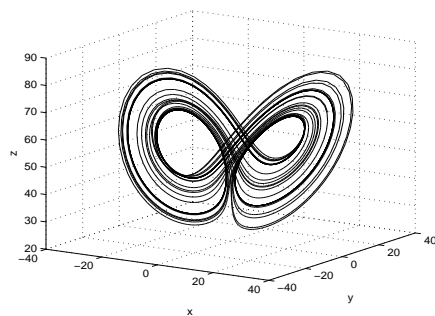


Fig. 1 ($r = 3.342$)Fig. 2 ($r = 3.837$)Fig. 3 ($r = 4.515$)Fig. 4 ($r = 4.617$)Fig. 5 ($r = 4.714$)Fig. 6 ($r = 4.928$)Fig. 7 ($r = 8.914$)Fig. 8 ($r = 10.921$)Fig. 9 ($r = 14.884$)Fig. 10 ($r = 16.964$)

Fig. 11 ($r = 24.714$)Fig. 12 ($r = 25.811$)Fig. 13 ($r = 29.713$)Fig. 14 ($r = 30.713$)Fig. 15 ($r = 30.713$)Fig. 16 ($r = 30.721$)Fig. 17 ($r = 31.896$)Fig. 18 ($r = 32.021$)

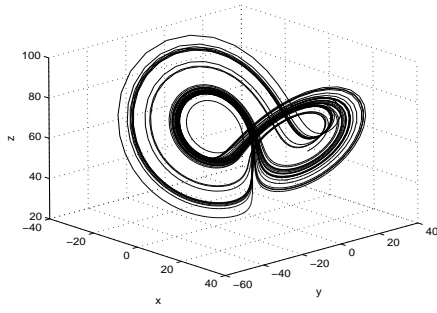


Fig. 19 ($r = 35.796$)

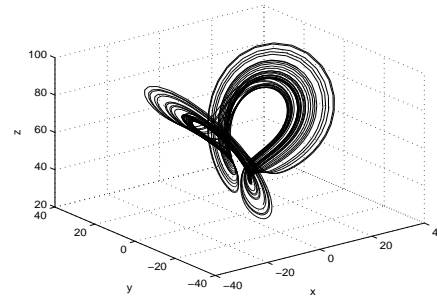


Fig. 20 ($r = 36.981$)

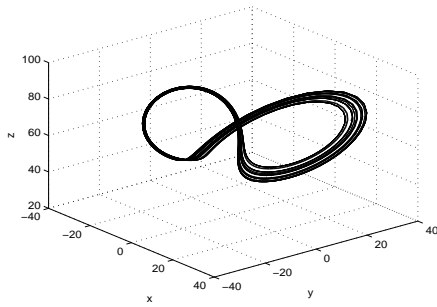


Fig. 21 ($r = 38.746$)

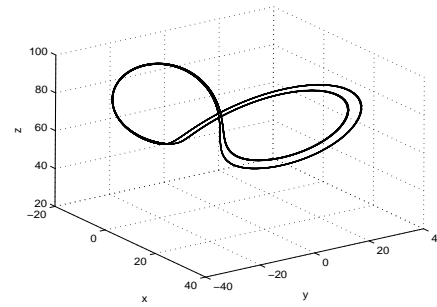


Fig. 22 ($r = 39.881$)

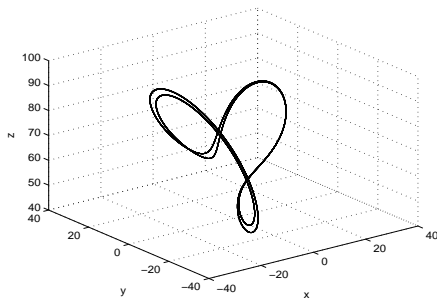


Fig. 23 ($r = 40.896$)

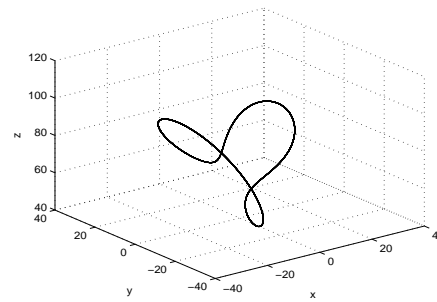


Fig. 24 ($r = 42.855$)

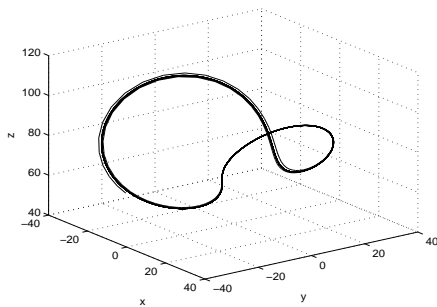


Fig. 25 ($r = 44.786$)

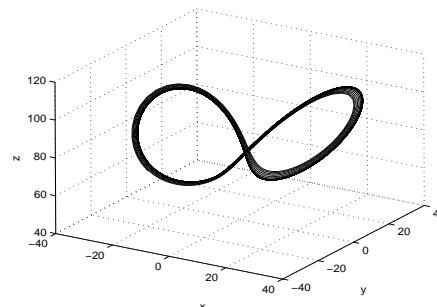
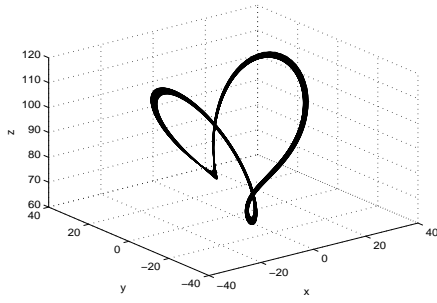
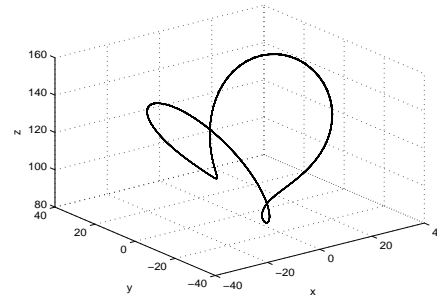
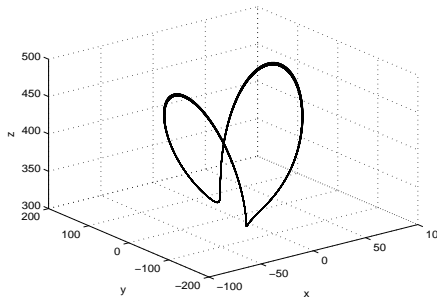
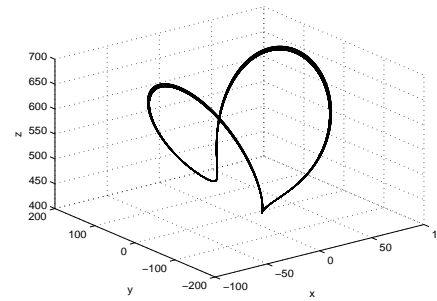
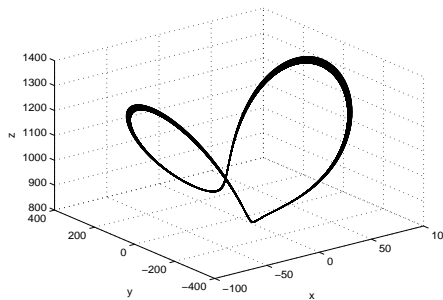
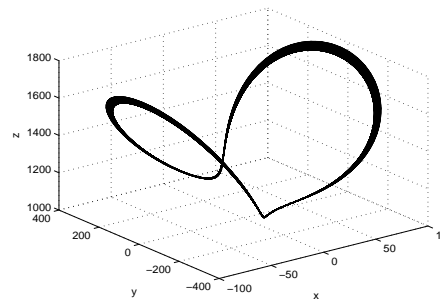
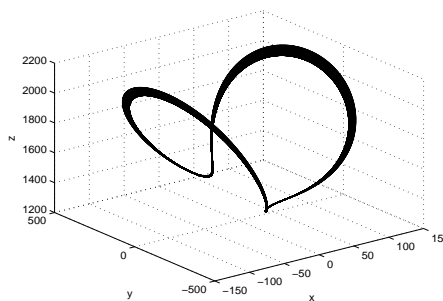
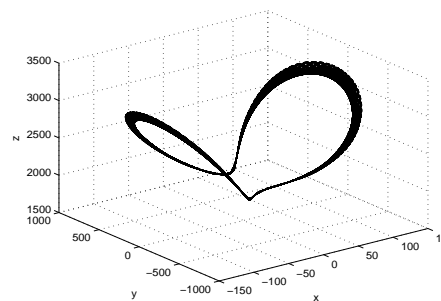


Fig. 26 ($r = 48.895$)

Fig. 27 ($r = 52.896$)Fig. 28 ($r = 68.893$)Fig. 29 ($r = 224.895$)Fig. 30 ($r = 324.894$)Fig. 31 ($r = 624.895$)Fig. 32 ($r = 824.894$)Fig. 33 ($r = 1204.895$)Fig. 34 ($r = 1504.894$)

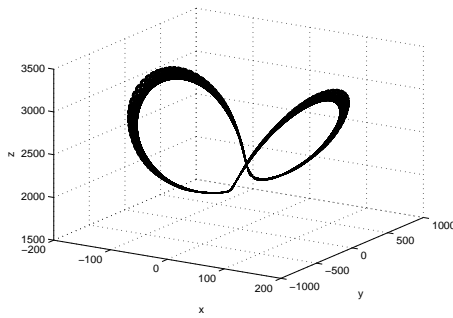


Fig. 35 ($r = 1505.843$)

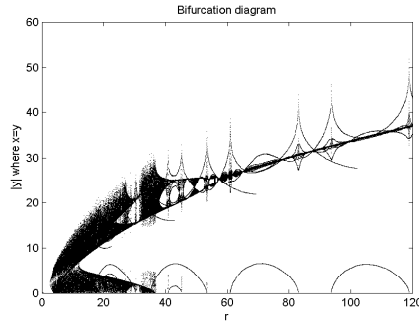


Fig. 36

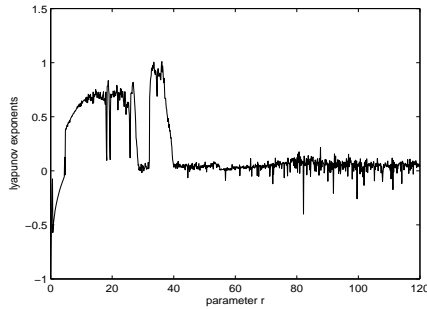


Fig. 37

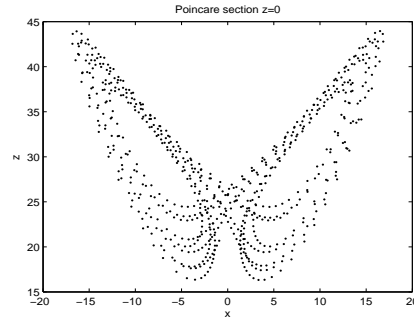


Fig. 38 ($r = 34.894$)

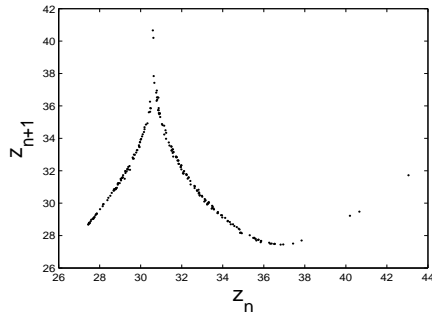


Fig. 39 ($r = 14.894$)

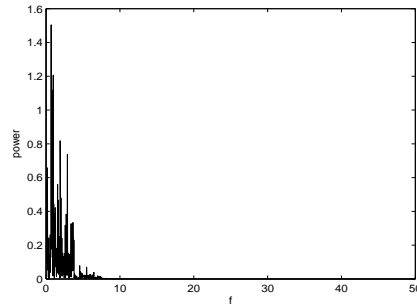


Fig. 40

The numerical results 1)–3) can be used to explain successive transitions phenomena of Couette-Taylor flow from Laminar flow to turbulence in the experiment, for example, in the regime $0 < r < r_1$ the only attractor is O , this represents a situation in which the fluid is at rest, this stable equilibrium regime correspond to Couette flow. The steady states P_{\pm} both represent time-independent convective flow patterns, this correspond to the Taylor vortices and the rotating waves. The quasi-periodic orbits in the Figs. 5–9 are with respect to modulated wavy Taylor vortices, strange attractor in the Fig. 10 correspond to turbulence (chaos), and so on. These simulation results indicate that the transition from stable equilibrium point \rightarrow unstable equilibrium point \rightarrow periodic \rightarrow quasi-periodic \rightarrow transient chaos \rightarrow chaos, similar to one of the experimental results of Gollub and Benson [1980]. Although our numerical result is not completely compatible with the experimental result, it is similar to the experimental result qualitatively. In order to check the behaviors of this low-dimensional

model, we have obtained a five-dimensional system for the same problem, the obtained results are very similar. The five-dimensional system also exhibits a period doubling scenario. The bifurcations occur at different Reynolds numbers. In both cases, the qualitative phenomena are essentially the same.

According to the numerical computation results and analysis, we present stability of the three-mode and corresponds to the actual flow of Couette-Taylor flow by the following table 4.1.

Table 4.1 Equilibrium points property of three-mode system and corresponds to the actual flow of Couette-Taylor flow

r -value	$0 < r < r_1$	As $r > r_1$ increases further		
equilibrium O	Stable node	Saddle node One direction is unstable, the other two directions are stability		
P^+ , P^-	No equilibrium	Stable node	Stable focus	Saddle point
Phase trajectory of system (2.1)	Tends to stable equilibrium O	Tends to stable equilibrium P^+ or P^-	spiral line Tends to P^+ or P^-	Unstable limit cycles subcritical Hopf bifurcation
the actual flow of C-T flow	Couette flow	the Taylor vortices and rotating traveling waves		irregular turbulent chaotic

5. Conclusions

This paper has studied a three-mode Lorenz-type system of the incompressible flow between two concentric rotating cylinders. Dynamical behaviors of the chaotic system, including the strange attractor, bifurcations, and some universal features of chaos behaviors have been investigated both theoretically and numerically by changing parameter r . Compared with the classical Lorenz system, our three-mode system differs only by the right-hand side for the x -derivative where is, as an addition, a term cyz , our three-mode system does not reproduce the qualitative features of Lorenz system from which it has been obtained as an extension, no stable attracting periodic orbit being present at high values of the parameter r , in some intervals hysteresis takes place between closed orbits and tori. Even if the three-mode model studied dose not reproduce the interesting phenomena of the Lorenz system, we think it is

also interesting by itself. In fact its phenomenology, studied quite in detail, appears so rich and varied to amply justify the present work.

REFERENCES

- [1] F. Chen, D. Y. Hsien, A Model Study of Stability of Couette Flow, *Comm. on. Applied Math. and Comp.*, 12:22–33, 1987.
- [2] H. Y. Wang, Dynamical Behaviors and Numerical Simulation of Lorenz Systems for The Incompressible Flow Between Two Concentric Rotating Cylinders, *International Journal of Bifurcation and Chaos*, 22(5):22-27, 2012.
- [3] H. Y. Wang, The chaos behavior and simulation of three model systems of Couette-Taylor flow, *Acta Mathematica Scientia*, 35(2):769–779, 2015.
- [4] C. M. Gassa Feugainga, O. Crumeyrollea, K. S. Yangb, I. Mutabazia, Destabilization of the CouetteCTaylor flow by modulation of the inner cylinder rotation, *European Journal of Mechanics - B/Fluids*, 719:14–46, 2013.
- [5] Richard J. A. M. Stevens Siegfried Grossmann, Roberto Verzicco, D. Lohse, Optimal Taylor-Couette flow: Direct numerical simulations, *Journal of Fluid Mechanics*, 34:267–284, 1998.
- [6] Olivier Czarny, Eric Serre, Identification of complex flows in Taylor-Couette counter-rotating cavities, *C. R. Acad. Sci. Paris t. 329, Serie II*, 727–733, 2001.
- [7] Pascal Chossat, Gerard Tooss, *The Couette-Taylor problem*, Springer Verlag, New York, 1994.
- [8] H. L. Swinney, J. P. Gollub, *Hydrodynamic, Instabilities and the Transition to Turbulence*, Springer Verlag, New York, 1981.
- [9] G. I. Taylor, Stability of a Viscous Liquid Contained Between Two Rotating Cylinders, *Phil. Trans. Roy. Soc., London*, A223: 289–343, 1923.
- [10] D. G. Thomas, B. Khomami, R. Sureshkumar, Nonlinear dynamics of viscoelastic Taylor-CCouette flow, effect of elasticity on pattern selection, molecular conformation and drag, *J. Fluid Mech.*, 620:353–C382, 2009.
- [11] C. D. Anderreck, S. S. Liu, and H. L. Swinney, Flow regimes in a circular Couette system with independent rotating cylinders, *J. Fluid Mech.*, 64:155–183,1986.
- [12] R. Temam, *Infinite dimensional dynamic system in mechanics and physics*, *Appl. Math. Sci.*, Springer Verlag, New York, 2000.
- [13] J. P. Gollub S. V. Benson, Many routes to turbulent convection, *J. Fluid Mech.*, 100:449, 1980.